

Structure Sensitivity of NO Adsorption on a Smooth and Stepped Pt(100) Surface

H. P. BONZEL, G. BRODÉN, AND G. PIRUG

Institut für Grenzflächenforschung und Vakuumphysik, Kernforschungsanlage Jülich, D-517 Jülich, Germany

Received July 6, 1977; revised January 24, 1978

The adsorption of NO was studied in the temperature range 300–500 K by low-energy electron diffraction (LEED), photoemission, and Auger electron spectroscopy on a smooth Pt(100) crystal exhibiting a 1×1 , 5×20 , or $\sqrt{29} \times \sqrt{170}$ structure, and a stepped Pt $[4(100) \times (111)]$ crystal with 1×1 or reconstructed surface. The initial sticking coefficient of NO on all surfaces was about 0.6 at 300 K. Adsorbed molecular NO on the Pt(100)- 1×1 surface gave rise to a sharp $c(2 \times 4)$ type LEED pattern. A structure model for this pattern was proposed on the basis of nonlinearly bonded NO molecules. On heating the adsorbed NO molecules dissociated on all surfaces; the onset of dissociation was approximately at 400 K independent of structure and steps. No adsorption of NO could be observed on reconstructed surfaces at $T > 380$ K. On the other hand, unreconstructed surfaces were able to adsorb NO molecularly at temperatures up to 410 K and dissociatively at $T = 423$ and 435 K for the smooth and stepped surface, respectively. Dissociative NO adsorption was also verified for a carbon stabilized Pt(100)- 1×1 surface at 473 K. We conclude that surface reconstruction can play a more significant role on NO adsorption kinetics than monatomic steps.

1. INTRODUCTION

The atomistic interpretation of structure sensitivity in chemisorption and heterogeneous catalysis is usually based on the concept of low coordination surface sites (1). In simple language these sites are made up of atoms whose coordination number is less than that of a surface atom located in a flat terrace. At the same time low coordination sites are thought to exhibit "dangling bonds" (2) which are active for adsorbing molecules from the gas phase. This type of structure sensitivity is in particular demonstrated by the particle size dependence of catalytic reaction rates and more recently by chemisorption studies on stepped single crystal surfaces (3).

Whereas the low coordination sites are generally isolated on the surface, it is also possible to extend the concept of structure sensitivity to a description of certain surface orientations which as a whole exhibit a special catalytic activity. In this context the so-called "reconstructed surfaces" play an important role. Examples of a possible connection between surface reconstruction and structure sensitivity are discussed in the literature (4, 5). It is most interesting that the Pt(100) oriented surface is a clear case where surface reconstruction is the cause of a marked structure sensitivity of chemisorption (6). This was demonstrated for O₂ and H₂ adsorption, and in this paper we will demonstrate the same effect for the dissociative adsorption of NO. At

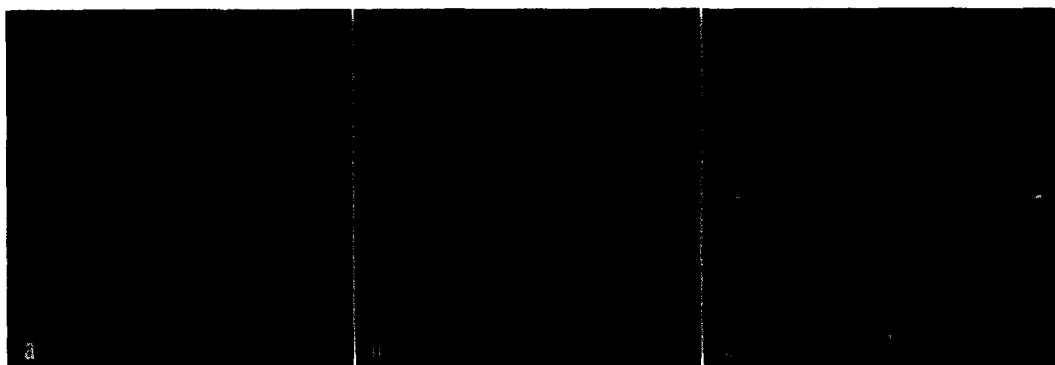


FIG. 1. LEED patterns of the clean Pt(100) surface: (a) 5×20 pattern, 21 eV; (b) $\sqrt{29} \times \sqrt{170}$ pattern, 21 eV; (c) 1×1 pattern, 49 eV.

the same time we compare the effect of atomic steps and reconstruction and conclude that in this case steps are of minor significance and reconstruction is of major significance for NO dissociative adsorption.

The results of this study provide supplementary information on the chemistry of NO on Pt which was the subject of various other publications (7-10). These earlier papers dealt primarily with the low temperature adsorption properties of NO on low-index Pt faces whereas the present work emphasizes the aspects of structure sensitivity and dissociative NO adsorption from the gas phase.

2. EXPERIMENTAL

The investigation was carried out in a stainless-steel, ultra-high vacuum system with a base pressure of 5×10^{-9} Pa. The analytical capabilities of this system were low-energy electron diffraction (LEED), Auger electron spectroscopy (AES), ultra-violet as well as X-ray photoemission spectroscopy (UPS and XPS), and quadrupole mass spectrometry. Additional features were an argon ion gun for surface cleaning, an ionization gauge for measuring the pressure, and a sample manipulator for x, y, z, ϕ motion of the sample. Further details of the system were published previously (7).

Two different crystals were cut from a

high purity Pt single crystal ingot. The first crystal had a (100) orientation to within 0.5° , the second was cut at an angle of 10° from the (100) orientation along the $[01\bar{1}]$ zone. According to Lang *et al.* (3) the latter crystal is designated Pt[4(100) \times (111)]. Thus the surface of this crystal (after cleaning and annealing) is characterized by terraces four atomic rows wide on the average and monatomic steps of (111) orientation. The platinum crystals were mounted on polycrystalline Pt foil and heated from the back side by electron bombardment. The temperature of the sample was measured by a Pt, Pt-10% Rh thermocouple spot welded to the sample edge.

The polished platinum crystals were cleaned *in situ* by ion bombardment and heated at 1000 K in O_2 atmosphere of 10^{-4} Pa and flashed to 1300 K. This treatment was carried out until AES scans of the total surface did not reveal any impurities. Typical impurities seen during the initial cleaning phase were C, Ca, P, K, and Na. The latter two could be observed mass spectrometrically during heating of the crystal (11). At temperatures above 900 K Na and K desorb from the surface as positive ions; acceleration of these ions by 50-70 eV is sufficient for them to penetrate the ionizer section of the mass spectrometer (11). There was no correlation between

the appearance of K and Na impurities and the various surface structures on Pt(100) observed during this investigation.

3. RESULTS

3.1. Reconstructed Pt(100) Surface

The well-annealed and clean Pt(100) surface is reconstructed and is characterized by *two* different structures, as first pointed out by McCarroll (11). The 5×20 structure is stable up to about 1070 K and transforms at higher temperatures irreversibly to the $\sqrt{29} \times \sqrt{170}$ structure. Figure 1a and b shows the LEED patterns corresponding to these two structures. In addition to the 5×20 and $\sqrt{29} \times \sqrt{170}$ structures the Pt(100) surface can also be brought into a nonreconstructed 1×1 state (Fig. 1c) whose stability is limited to temperatures below about 420 K (12). Thus the Pt(100) surface exhibits three structures with increasing stability, namely, 1×1 , 5×20 , and $\sqrt{29} \times \sqrt{170}$. The latter two exist in two domains rotated 90° to each other.

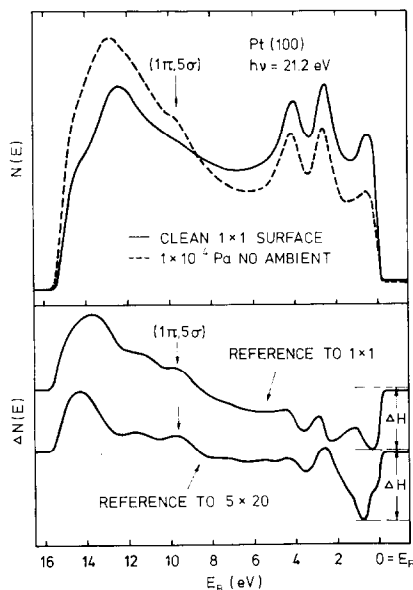


FIG. 2. UPS spectrum of molecular NO adsorbed on Pt(100); note the peak in the difference curve $\Delta N(E)$ due to $1\pi 5\sigma$ molecular orbitals.

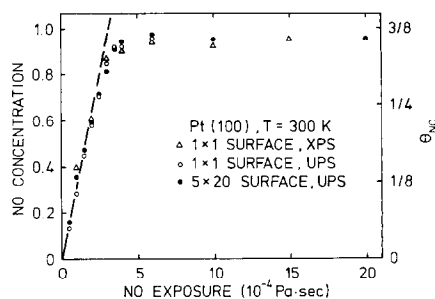


FIG. 3. Kinetics of NO adsorption on Pt(100) at 300 K.

The adsorption of NO on the 5×20 or the $\sqrt{29} \times \sqrt{170}$ surface occurs readily at $T < 345$ K. The LEED patterns change during adsorption from that of the reconstructed surface to a 1×1 pattern plus fuzzy ($\frac{1}{2} \frac{1}{4}$) and ($\frac{1}{4} \frac{3}{4}$) spots (7). Under these conditions NO is adsorbed in molecular form as can be most easily seen by the corresponding UPS spectra. A typical NO spectrum for $h\nu = 21.2$ eV is shown in Fig. 2 including the difference $\Delta N(E)$. This difference spectrum is characterized by the NO molecular orbital resonance at 9.7 eV below E_f and a strong decrease in emission at about 1 eV below the Fermi level, ΔH . These spectra are in agreement with previous work (7, 10). A quantitative study of NO adsorption showed that the decrease ΔH near E_f was proportional to the intensity of the oxygen 1s level (measured by XPS) and the molecular orbital level at 9.7 eV. Therefore, ΔH was taken as a relative measure of the amount of adsorbed molecular NO. Figure 3 shows a plot of ΔH and the O(1s) peak intensity versus NO exposure at 300 K, which is a good representation of the adsorption kinetics of NO. Based on the calibration point $\theta = \frac{3}{8}$ at saturation (13), we evaluated the initial sticking coefficient s_0 of NO on the reconstructed Pt(100) surface to be 0.6.

Preadsorbed molecular NO dissociates on Pt(100) during heating (7). An estimate of the beginning of NO dissociation was

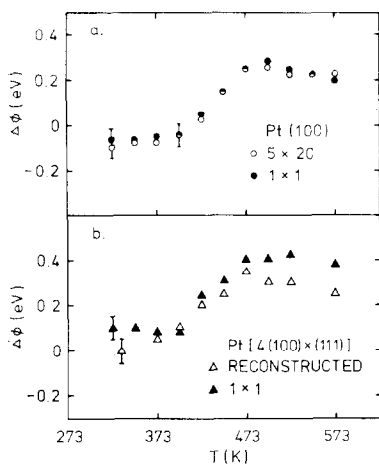


FIG. 4. Work function change $\Delta\phi$ versus temperature for successively heated, NO saturated Pt crystals. (a) Smooth Pt(100) crystal; (b) stepped Pt crystal.

obtained by successive heating of the NO saturated crystal to a temperature T and measuring the resulting change in work function, $\Delta\phi$, due to adsorbed atomic oxygen. The rate of heating was approximately 1.2 K sec^{-1} and kept constant. Figure 4a shows a set of $\Delta\phi$ versus T data for the Pt(100) surface which originally had been in the 5×20 state and after NO adsorption been converted to a 1×1 state. Assuming that the beginning of a

change in $\Delta\phi$ indicates the dissociation of adsorbed NO one evaluates the onset temperature of NO dissociation to be around 400 K.

Attempts to adsorb NO on the 5×20 surface above $T = 380 \text{ K}$ were unsuccessful. No evidence for either molecular or dissociated NO was found at these temperatures for NO exposures up to $2 \times 10^{-3} \text{ Pa sec}$.

3.2. Pt(100) - 1×1 Surface

The clean, unreconstructed 1×1 surface (12) was reproducibly obtained by the following procedure: NO adsorption at $T < 340 \text{ K}$ up to saturation, slow heating to 470 K, $1 \times 10^{-3} \text{ Pa sec}$ of H_2 at $T \leq 340 \text{ K}$, brief heating to 390 K. During this sequence of steps NO dissociates on the Pt(100) surface leaving atomic adsorbed oxygen behind; this oxygen is reacted off with H_2 and finally excess adsorbed hydrogen is desorbed. At this stage LEED always showed a sharp 1×1 pattern (Fig. 1c) and the surface was clean by AES.

The low temperature adsorption of NO on the 1×1 surface was very similar to that on the reconstructed surface. The adsorption kinetics of NO are included in Fig. 3 together with those for the re-

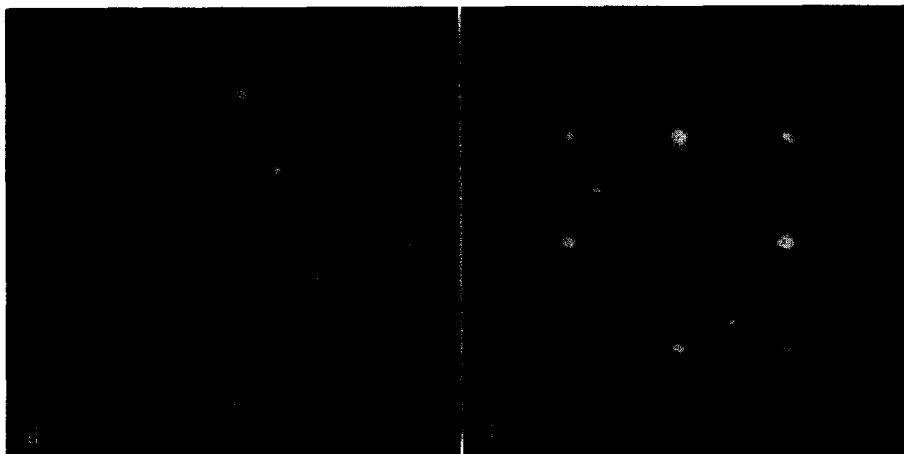


FIG. 5. The $c(2 \times 4)$ LEED patterns of NO adsorbed on the unreconstructed Pt(100)- 1×1 surface. (a) 65 eV; (b) 110 eV.

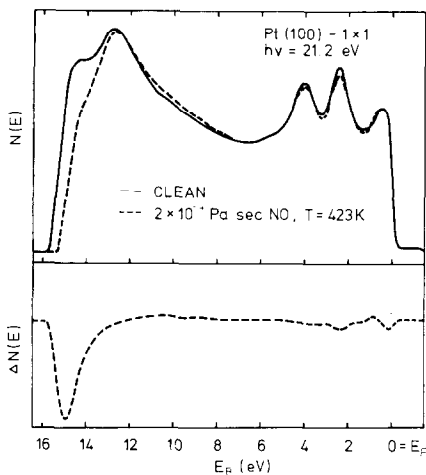


FIG. 6. UPS spectra of clean Pt(100)- 1×1 surface and after dissociative NO adsorption at 423 K. Note the change in work function of ~ 0.35 eV.

constructed surface yielding $s_0 = 0.6$. No evidence of dissociative NO adsorption at low temperature was found. The adsorption of molecular NO on the 1×1 surface gave rise to a sharp $c(2 \times 4)$ LEED pattern, shown in Fig. 5a and b. It should be noted that the pattern is not a simple $c(2 \times 4)$ because the $(0\frac{1}{2})$ and $(1\frac{1}{2})$ spots are lower in intensity than the $(\frac{1}{2}\frac{1}{4})$ and $(\frac{1}{2}\frac{3}{4})$ spots (of one domain). Slow heating

of the adsorbed NO layer caused eventual NO dissociation to occur, indicated by work function changes (Fig. 4a). The onset of NO dissociation was within error the same as for the (originally) 5×20 surface.

On the other hand, NO adsorption on 1×1 at elevated temperatures behaved quite differently. First, it was possible to adsorb molecular NO at temperatures as high as 410 K. Second, in the range 400–420 K both molecular *and* dissociative NO adsorption took place. Figure 6 shows UPS data (21.2 eV) for a clean 1×1 surface and after exposing this surface to 2×10^{-4} Pa sec of NO at a sample temperature of 423 K. The difference spectrum $\Delta N(E)$ does not indicate the presence of molecular NO but the $N(E)$ curves clearly show an increase in work function of 0.35 eV which is due to dissociated oxygen. The latter was in addition detected by AES and XPS, while nitrogen could not be detected after NO dissociation.

The test for dissociative NO adsorption on the clean 1×1 surface could only be carried out in the vicinity of 420 K. This temperature was still low enough for the 1×1 surface not to transform to the more stable 5×20 structure, and high enough for dissociative NO adsorption to occur.

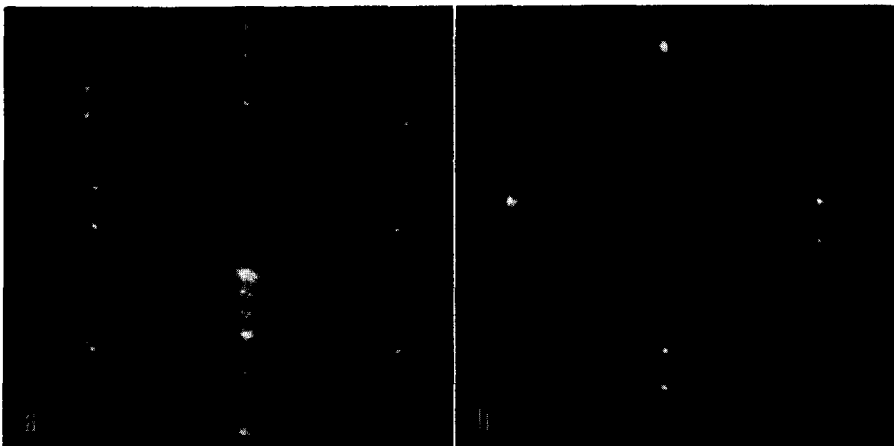


FIG. 7. LEED pattern of the clean Pt[4(100) \times (111)] surface. (a) "Reconstructed," 56 eV; (b) unreconstructed 1×1 , 58 eV.

3.3. Pt(100)—Carbon Contaminated

It is known (12, 14) that carbon stabilizes the unreconstructed 1×1 surface of Pt(100). This property of carbon was utilized here in order to check for dissociative NO adsorption at temperatures higher than 420 K. The 5×20 surface was exposed to 5×10^{-4} Pa sec of acetylene and then heated to 770 K. Due to the adsorption of acetylene the surface changes into a 1×1 configuration while the brief anneal at 770 K causes the acetylene to dehydrogenate completely. The result is a carbon-stabilized 1×1 surface which does not transform to the 5×20 surface below about 900 K. The ratio of the carbon to the Pt(238 eV) Auger peak was 0.24 in this case corresponding to an approximate carbon coverage of 0.3.

The adsorption of NO at 473 K on this carbon-stabilized 1×1 surface was clearly dissociative as evidenced by UPS data ($\Delta\phi$ change; absence of molecular orbital peaks) and AES. In addition some carbon was reacted from the surface due to the presence of atomic oxygen. This effect was seen by a decrease in the carbon Auger peak at $T = 473$ K and repeated NO exposures.

In a control experiment the carbon-contaminated surface was heated to 1090 K and thus converted to a 5×20 surface. This carbon-contaminated surface was also exposed to 1×10^{-3} Pa sec of NO at 473 K but no changes in the UPS spectrum were noted nor was adsorbed oxygen or a loss of carbon detected by AES. Therefore, not the presence of surface carbon but the unreconstructed state of the Pt(100) surface is responsible for the dissociative adsorption of NO at elevated temperatures.

3.4. Pt[4(100) \times (111)] Surface

This Pt crystal exhibited a reconstructed surface with a regular array of monatomic steps quite analogous to other misoriented Pt crystals studied previously (3). About

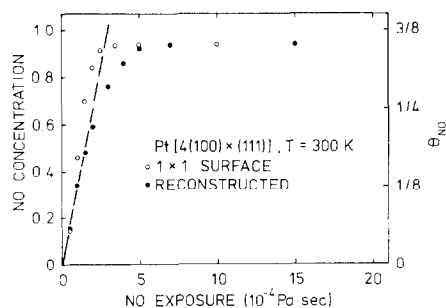


FIG. 8. Kinetics of NO adsorption on the stepped Pt crystal at 300 K.

every fourth row of atoms in the [110] direction represents a crystallographic step such that the density of step atoms is about 25%. The resulting terraces four atom rows wide are ideally too narrow for the unit cell of the 5×20 structure (15) unless coherent growth of this structure over several terraces would occur. However, this is very unlikely because neighboring terraces are out of phase; rather a new superstructure develops modulated by the high step density. The corresponding LEED pattern of this structure is illustrated in Fig. 7a. Note that only a single domain is observed for the stepped surface, consistent with a large unit cell. The occurrence of single domain patterns was also seen for Pt(100) surfaces with low step density, such as a Pt[9(100) \times (111)] surface.

The 1×1 structure of the stepped Pt crystal was generated in the same manner as for the smooth Pt(100) crystal. The LEED pattern for the 1×1 surface is shown in Fig. 7b where the spot splitting characteristic for steps can now be clearly seen. The width of the splitting was found to be consistent with the 10° tilt angle at which the crystal was cut.

Low temperature NO adsorption characteristics on the stepped reconstructed Pt crystal were similar to those for the Pt(100)- 5×20 and $\sqrt{29} \times \sqrt{170}$ structures. In particular the kinetics of molecular NO adsorption, again plotted as ΔH versus NO exposure in Fig. 8, were the

same within the accuracy of these measurements, resulting in an initial sticking coefficient of 0.6. The onset of dissociation, of molecularly adsorbed NO (Fig. 4b) was near 400 K and thus indistinguishable from the data of Fig. 4a. No dissociative adsorption of NO from the gas phase could be detected at $T \geq 420$ K on the reconstructed surface.

The corresponding low temperature adsorption data for the 1×1 surface are also presented in Figs. 4 and 8. The initial sticking coefficient s_0 of NO seems to be slightly higher than 0.6 whereas the onset of NO dissociation is indistinguishable from that of the reconstructed surface.

Before we present the results for NO adsorption on the 1×1 surface at elevated temperature, we will briefly take a look at the stability of the 1×1 surface for the smooth and stepped surface. As shown previously (12), the UPS difference spectrum between the clean 1×1 and the reconstructed surface of Pt(100) exhibits a narrow emission peak at 0.2 eV below the Fermi level. This peak is characteristic of

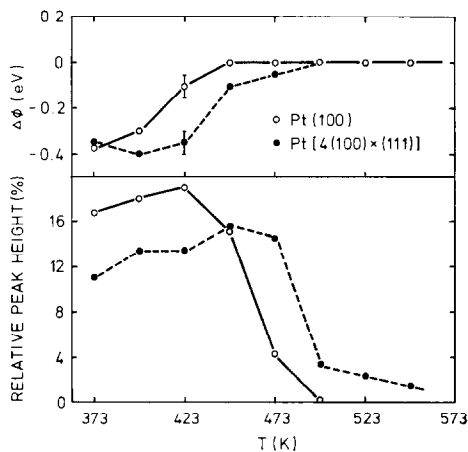


FIG. 9. (a) Work function change $\Delta\phi$ versus temperature for the unreconstructed surfaces, after NO dissociation and hydrogen reduction. (b) Relative peak height at the Fermi level versus temperature for the unreconstructed surfaces; the peak height is taken as a measure of the stability of the unreconstructed surface.

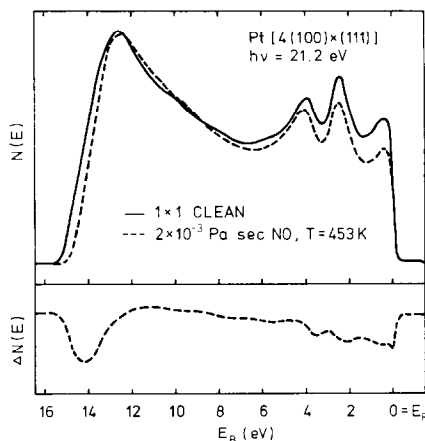


FIG. 10. UPS spectra of the clean unreconstructed, stepped Pt surface and after dissociative NO adsorption at 453 K. Note the change in $\Delta\phi$ of about 0.3 eV.

the 1×1 surface and probably represents a surface state (or resonance). The height of this peak, h , relative to the emission at the Fermi level of the unreconstructed surface, H , is of the order of 19% for Pt(100)- 1×1 . The 1×1 structure of the stepped surface also had a similar peak in the difference spectrum with a relative peak height of about 15%.

A measure of the stability of the 1×1 surface was obtained in the following experiment. During the last step in preparing the clean 1×1 surface the sample was heated successively to a temperature T and $\Delta\phi$ as well as the relative peak height h/H of the surface state were measured. Figure 9 shows the result for both the smooth and stepped Pt(100)- 1×1 surface. The $\Delta\phi$ changes are a result of the changing hydrogen coverage. Note that hydrogen desorption occurs at a higher temperature on the stepped than on the smooth surface.

Furthermore the starting temperature for the decrease in h/H is about 420 K for Pt(100)- 1×1 and 470 K for the Pt[4(100)×(111)]- 1×1 surface. Thus the presence of steps has a stabilizing effect on the 1×1 surface somewhat similar to that of carbon in section 3.3.

Because of the 1×1 structure stabilization by steps the test for dissociative NO adsorption was carried out at 453 K. The 1×1 surface was exposed to 2×10^{-3} Pa sec of NO at this temperature. The UPS spectra in Fig. 10 indicate a $\Delta\phi$ change of 0.4 eV and a lack of evidence of molecular NO. The presence of adsorbed oxygen was verified by AES. Therefore, dissociative adsorption of NO takes place on the stepped 1×1 surface at 453 K.

4. DISCUSSION

The Pt(100) surface is fairly unique in that it can exist in three different surface structures epitaxed to the same bulk structure. Whereas the 5×20 surface has been observed by several authors (11, 16), the more complex $\sqrt{29} \times \sqrt{170}$ surface was reported by Palmberg (17) and McCarroll (11). This structure is clearly the most stable one of all three since it does not convert back to the 5×20 or 1×1 except through gas adsorption or ion sputtering. It is now fairly well accepted that the 5×20 structure corresponds to a nearly hexagonal monolayer of Pt atoms on top of the (100) bulk lattice (15, 18). It is conceivable that the process of reconstruction which leads to the 5×20 structure and which is driven by a lowering of the total surface free energy, has not gone to completion. At the higher annealing temperature of 1100–1300 K the process of reconstruction may not be limited to the first layer but may penetrate deeper into the lattice yielding perhaps an epitaxially reconstructed seldedge of 2–3 layers thick. A more detailed analysis of the $\sqrt{29} \times \sqrt{170}$ LEED pattern will have to show whether such a hypothesis is reasonable or not.

The possibility of having three different structural arrangements of surface atoms on the same bulk crystal makes the Pt(100) surface a particularly interesting candidate for an investigation of the structure sensitivity in chemisorption and catalysis. In

addition this structural multiplicity can be increased by introducing monatomic steps onto the surface. For the adsorption of NO we can distinguish three characteristic processes: (a) molecular adsorption of NO, (b) dissociation of adsorbed molecular NO, and (c) dissociative adsorption of NO from the gas phase.

Our investigation shows that processes (a) and (b) are not very critical tests of structural sensitivity in this case since the data in Figs. 3, 4, and 8 indicate first, that the rate of molecular NO adsorption at low temperature is independent of structure and steps, and second, that the onset temperature of NO dissociation is also independent of the original structure and steps. In this context it is necessary to point out that the initial $\Delta\phi$ values (Fig. 4a and b) are affected by the accuracy of the measuring procedure (~ 0.1 eV) and, in the case of the unreconstructed surfaces, by the presence of a residual amount of hydrogen from the preparation procedure.

A genuine structure sensitivity is seen with experiment (c). Here a large difference in behavior is documented by Figs. 6 and 10 which prove the dissociative adsorption of NO at 423 and 453 K for the unreconstructed Pt(100) and Pt[4(100) \times (111)] surface, respectively. These data are supported by AES and XPS detection of adsorbed oxygen. The reconstructed surfaces, on the other hand, were not able to dissociate NO from the gas phase at these or higher temperatures.

Thus the primary role of steps in our case seems to be the stabilization of the 1×1 surface and thus an extension of the temperature range in which dissociative NO adsorption can take place. The same role is played by adsorbed carbon, with the only difference that the 1×1 surface is stable at even higher temperatures, up to ~ 900 K.

This 1×1 structure stabilization effect by steps and/or carbon could be important for the surface chemistry of small supported

Pt particles. If these particles with a diameter of 10–50 Å exhibit (100) oriented facets it might be significant that the surface structure of these facets would not be reconstructed in order to utilize the high specific activity of the Pt(100)– 1×1 surface. Because of the small size of these particles these surfaces might be vicinal rather than low index and thus contain steps which would stabilize the 1×1 structure. The same could be accomplished by carbon, an everpresent impurity under catalysis conditions involving hydrocarbons.

In order to rationalize the structure sensitivity of dissociative NO adsorption on Pt(100) we proposed previously (7) that NO dissociation is either activated ($E_{\text{dis}} > E_{\text{des}}$) or that the activation energy of dissociation varies with surface structure. It now seems that a combination of these ideas might provide a proper description of the facts. Figure 11 shows two adsorption potentials for NO, one for Pt(100)– 5×20 and the other for Pt(100)– 1×1 . The following arguments and additional observations will serve to support the existence of these potentials:

(i) Dissociative NO adsorption does not take place on the 5×20 surface; therefore the dissociation of NO on this surface is activated with an energy Q_a .

(ii) The initial sticking coefficient of molecular NO on the 5×20 surface decreases rapidly with increasing temperature. At ≈ 400 K very little molecular NO could be adsorbed in contrast to the 1×1 surface where the initial sticking coefficient at 400 K was unchanged from that measured at 300 K. Therefore, the activation energy of desorption, E'_{des} , of NO from the 5×20 surface might be smaller than that for the 1×1 surface, E_{des} .

(iii) Dissociation of adsorbed NO on the 1×1 surface is easily accomplished as well as dissociative adsorption at 420 K on the 1×1 surface; therefore $E_{\text{dis}} < E_{\text{des}}$ for the 1×1 surface.

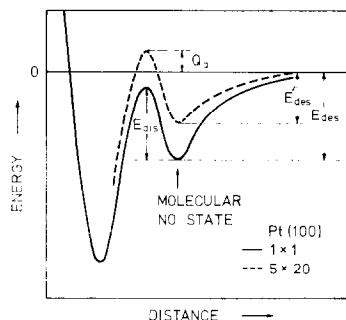


FIG. 11. Proposed energy potentials for NO adsorption on a reconstructed and 1×1 type surface of Pt(100).

These facts (i)–(iii) taken together allow the construction of the qualitative potentials shown in Fig. 11 for the two surface structures 5×20 and 1×1 . The essential feature is that during low temperature molecular NO adsorption a transformation $5 \times 10 \rightarrow 1 \times 1$ takes place. This structural transformation causes locally a concomitant change in the adsorption potential from the 5×20 type to the 1×1 type. The Pt(100)– 1×1 surface therefore behaves quite similarly to a polycrystalline Pt foil where a detailed study of NO adsorption also showed $E_{\text{dis}} < E_{\text{des}}$ in the low NO coverage range (19).

Finally we take a look at the LEED pattern of molecular NO and the corresponding NO coverage. XPS measurements of the $0(1s)$ level have shown (13) that the NO coverage at saturation is lower than the CO coverage under similar conditions. More recent quantitative studies of the same problem supported this result and indicated a saturation coverage of molecular NO between 0.38 and 0.40. The LEED pattern at saturation coverage as well as at an early stage of NO adsorption ($\sim 1 \times 10^{-4}$ Pa sec) shows a $c(2 \times 4)$ type pattern (Fig. 4a and b) which ideally gives rise to a coverage 0.25. However, this particular NO $c(2 \times 4)$ pattern is not of the simple kind since considerable intensity modulations in the $(\frac{1}{2} 0)$ and $(\frac{1}{2} 1)$ spots can be noticed. In addition the coverage

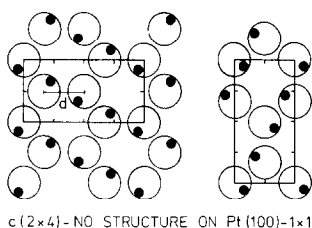


FIG. 12. Structure model for $c(2 \times 4)$ type NO layer on Pt(100)- 1×1 .

at this point should certainly exceed 0.25. A structure model for this NO pattern should take into account these two features.

Another point which has to be considered in proposing a structure model for the adsorbed NO layer has to do with the result that the adsorbed NO molecules are probably bonded in a kinked configuration (7). In this configuration oxygen is presumably an electron acceptor and negatively charged. Therefore, one may expect repulsive interactions between adsorbed NO molecules with a highly orienting torque. A structure model which (a) minimizes repulsive interaction between NO^- species, (b) gives rise to a $c(2 \times 4)$ type LEED pattern, and (c) has a saturation coverage higher than 0.25, namely 0.5, is shown in Fig. 12. In this model the O^- centers of the molecules (indicated by the black dots) are arranged in such a way that the Coulombic forces between them are near equilibrium. The proposed structure in Fig. 12 can exist in two domains rotated 90° to each other. A kinetic diffraction pattern of the structure in Fig. 12 obtained by laser diffraction (20) shows in fact much higher intensities for the $(\frac{1}{4} \frac{1}{2})$ and $(\frac{3}{4} \frac{1}{2})$ spots than for the $(\frac{1}{2} 0)$ and $(\frac{1}{2} 1)$ spots. On the other hand, if we decrease the distance d between two neighboring NO molecules (Fig. 12) the intensities of the $(\frac{1}{2} 0)$ and $(\frac{1}{2} 1)$ beams become even weaker. These spots have exactly zero intensity when d is equal to the nearest neighbor distance of Pt atoms in the Pt(100)- 1×1 surface. However, the intensities of these spots are in reality not quite zero (at least not for the higher order beams, Fig. 5b) so that the real d

is slightly larger than the nearest neighbor distance of Pt atoms. Further studies, in particular by electron energy loss spectroscopy, are aimed at identifying the adsorption site and angle of NO on Pt(100)- 1×1 as well as finding further support for the proposed LEED structure model of the adsorbate layer (21).

ACKNOWLEDGMENTS

We are indebted to H. Ibach and E. E. Latta for valuable discussion and comments on the manuscript.

REFERENCES

1. Taylor, H. S., *Proc. Roy. Soc. A* **108**, 105 (1925).
2. Schlosser, E. G., "Heterogene Katalyse." Verlag Chemie, Weinheim, 1972.
3. Lang, B., Joyner, R. W., and Somorjai, G. A., *Surface Sci.* **30**, 454 (1972).
4. Boudart, M., *J. Vac. Sci. Technol.* **12**, 329 (1975).
5. Taylor, K. C., Sinkevitch, R. M., and Klimisch, R. L., *J. Catal.* **35**, 34 (1974).
6. Helms, C. R., Bonzel, H. P., and Kelemen, S., *J. Chem. Phys.* **65**, 1773 (1976).
7. Bonzel, H. P., and Pirug, G., *Surface Sci.* **62**, 45 (1977).
8. Comrie, C. M., Weinberg, W. H., and Lambert, R. M., *Surface Sci.* **57**, 619 (1976).
9. Ibach, H., and Lehwald, S., IV. Rolla Conference on Surface Properties, University of Missouri, Rolla, August 1977.
10. Bonzel, H. P., and Fisher, T. E., *Surface Sci.* **51**, 213 (1975).
11. McCarrroll, J. J., *Surface Sci.* **53**, 297 (1975) and private communication.
12. Bonzel, H. P., Helms, C. R., and Kelemen, S., *Phys. Rev. Lett.* **35**, 1237 (1975).
13. Brodén, G., Pirug, G., and Bonzel, H. P., *Surface Sci.*, **72**, 45 (1978).
14. Somorjai, G. A., *Catal. Rev. Sci. Eng.* **7**, 87 (1972).
15. Fedak, D. G., and Gjostein, N. A., *Surface Sci.* **8**, 98 (1967).
16. Morgan, A. E., and Somorjai, G. A., *J. Chem. Phys.* **51**, 3309 (1969).
17. Palmberg, P. W., in "The Structure and Chemistry of Solid Surfaces" (G. A. Somorjai, Ed.), p. 29-1. Wiley, New York, 1969).
18. Heinz, K., Heilmann, P., Müller, K., *Z. Naturf.* **32a**, 28 (1977).
19. Pirug, G., and Bonzel, H. P., *J. Catal.* **50**, 64 (1977).
20. Fedak, D. G., Fischer, T. E., and Robertson, W. D., *J. Appl. Phys.* **39**, 5658 (1968).
21. Pirug, G., and Hopster, H., to be published.